ISSN (Print) 1226-1750
ISSN (Online) 2233-6656
Journal of Magnetics 28(4), 385-391 (2023) https://doi.org/10.4283/JMAG.2023.28.4.385

Mössbauer and Magnetic Properties of Fe-Cu-Nb-Si-B Amorphous Powders for High Frequency Applications

Sung Yong An[1,2]*

[1]*Seoul Business School, aSSIST University, 46 Ewhayeodae 2-gil, 03767 Seodaemun-gu, Seoul, Republic of Korea*
[2]*School of Business, Franklin University Switzerland, Via Ponte Tresa 29, 6924 Sorengo, Switzerland*

(Received 11 September 2023, Received in final form 11 September 2023, Accepted 24 October 2023)

In this study, amorphous powders of Fe-Cu-Nb-Si-B composition were synthesized through gas and water atomization techniques utilizing industrial-grade raw materials. Subsequently, these powders underwent a sieving process to achieve a particle size classification under 53 μm, with an average particle size (D50) of 26 μm. The prepared powder underwent a series of heat treatments at temperatures of 450 °C, 475 °C, 500 °C, 525 °C, and 550 °C to investigate changes in its crystallographic structure, utilizing X-ray diffractometry (XRD). Simultaneously, magnetic properties were assessed through Mössbauer spectroscopy and vibrating sample magnetometry (VSM). The observed phase transformation progressed from amorphous to crystalline as the heat treatment temperature increased. An entirely amorphous phase was maintained up to 500 °C, beyond which a mixed amorphous and crystalline phase emerged at higher temperatures. Mössbauer analysis revealed that, at 525 °C, approximately 39 % of the material remained in an amorphous state, while 61 % had transitioned into a crystalline phase. Further, at 550 °C, the amorphous fraction decreased to approximately 31 %, while the crystalline fraction increased to 69 %. The crystalline phase was identified as consisting of α-Fe, α-FeSi, Fe_2Si, Fe_3Si at *A*-sites, Fe_3Si at *B*-sites, and Fe_2B sites in the case of the 550°C heat treatment. With increasing heat treatment temperature, the saturation magnetization exhibited an initial increase, followed by a decline from 550 °C onward. This decline coincided with the decomposition of the material into multiple crystalline phases. Moreover, the Curie temperature was determined to be T_C1=845 K and T_C2=955 K, indicating two distinct magnetic transition temperatures in the studied material.

Keywords : ^{57}Fe Mössbauer spectroscopy, Fe-Cu-Nb-Si-B, amorphous powder, power inductor

1. Introduction

Magnetic materials play a pivotal role in the development of modern electronic devices, particularly in the field of high-frequency applications where minimizing eddy current losses is of paramount importance. Among these materials, amorphous powders composed of Fe-Cu-Nb-Si-B have garnered significant attention due to their potential to mitigate core losses and exhibit superior saturation magnetization compared to spinel ferrites, making them ideal candidates for chip power inductors operating at frequencies exceeding 1 MHz [1-6].

Spinel ferrites have traditionally been the preferred choice for chip power inductors. However, they lag behind amorphous magnetic materials in terms of saturation magnetization. Chip power inductors designed for high-frequency applications exceeding 1 MHz are indispensable components in power management ICs and DC-DC converters, where high current-carrying capacity and low R_{DC} resistance are imperative [7-9]. Nonetheless, amorphous magnetic materials face challenges when employed in high-frequency applications due to their relatively high eddy current losses. To circumvent this issue, it has been proposed that using a higher proportion of amorphous metal powders with lower resistivity than crystalline amorphous counterparts could effectively reduce eddy current losses. However, utilizing metal magnetic powders alone is impractical for high-frequency applications due to the Snoek's limit, rendering metal magnetic powders unsuitable for frequencies exceeding the MHz range [10-12].

A promising solution to extend the usability of metal magnetic powders into higher frequency ranges involves their incorporation into polymer matrices, such as epoxy

*Corresponding author: Tel: +82-10-4340-2344
Fax: +82-504-401-8679, e-mail: sung.an@stud.assist.ac.kr

binders. When formulated as composites, these materials can shift their magnetic resonance frequencies to align with high-frequency ranges, enabling their application as essential electronic components within this frequency domain [8, 13].

Researchers have sought to enhance the magnetic properties of amorphous metal powders through controlled heat treatments, with a particular focus on temperatures below the onset of crystallization. Identifying the temperature at which crystallization initiates is vital for optimizing the magnetic characteristics of these materials. Furthermore, investigations have delved into the magnetic property alterations and phase transitions occurring during the transition from amorphous to crystalline states [14-16].

In this study, we investigate the magnetic property evolution of Fe-Cu-Nb-Si-B amorphous powders with respect to heat treatment temperatures and explore their suitability for high-frequency applications. The crystallographic and magnetic properties of the samples are meticulously analyzed using X-ray diffraction (XRD), vibrating sample magnetometry (VSM), scanning electron microscopy (SEM), and Mössbauer spectroscopy (MS). Through this research, we aim to shed light on the potential of amorphous metal powders in high-frequency electronic components.

2. Experiments

The basic powders used in this research were commercial atomized Fe-Cu-Nb-Si-B amorphous powder with average particle sizes of 26 μm. The Fe-Cu-Nb-Si-B had a Cu content of 1.3 wt%, Nb content of 5.69 wt%, Si content of 8.03 wt.% and a B content of 1.77 wt.%. The Fe-Cu-Nb-Si-B powders were heat treated in a vacuum electric furnace from 450 ℃ to 550 ℃ at 25 ℃ intervals, with each heat treatment time being 30 minutes. The average particle size (D50) of the prepared powders was precisely determined using a particle size analyzer (PSA, MKT LA-950). Furthermore, the powders were comprehensively characterized for particle size distribution and morphological features using a scanning electron microscope (SEM, Hitachi S3500). The crystal structure and purity of the maghemite nanopowders were characterized using x-ray diffraction (XRD) with Cu$K\alpha$ radiation on a Philips x-ray diffractometer. The magnetic properties, including coercivity and magnetic moment, were measured by a vibrating sample magnetometer (VSM, Lake Shore 7300) under an applied magnetic field of 10 kOe. The Mössbauer spectra were recorded using an electrodynamic acceleration spectrometer at room temperature, with a 40mCi ^{57}Co source in Rh metal serving as the γ-ray source. The permeability at high frequencies was measured at frequencies from 0.1 MHz to 110 MHz using an impedance analyzer (Agilent, model 4294A), where the sample was made into a toroidal shape with 2.5 wt% of epoxy binder.

3. Results and Discussion

A particle size analyzer was used to analyze the average grain size of the amorphous powders of Fe-Cu-Nb-Si-B and the results of the analysis are shown in Fig. 1. The metal powders showed a size distribution of 4 to 100 um. The analysis of the particle size distribution of the powders showed that the median particle size, represented by D50, was about 26 micrometers. In addition, the particle morphology was examined, and it was found that spherical shapes with a near spherical geometry prevailed, which is also inserted in Fig. 1. These results suggest that the powder has a wide range of sizes and exhibits a relatively spherical particle structure, which may have important implications for its behavior and applications in various processes, including those involved in this study.

To investigate the thermal response of Fe-Cu-Nb-Si-B amorphous metal magnetic powder, a series of heat treatment experiments were conducted. The powder specimens were subjected to annealing in a vacuum oven at temperatures of 450 °C, 475 °C, 500 °C, 525 °C, and 550 °C, each for a duration of 30 minutes. Figure 2 presents the results obtained from X-ray diffraction (XRD) analyses performed on Fe-Cu-Nb-Si-B. The XRD analysis of the untreated powder displayed a distinct pure amorphous X-ray phase. As the heat treatment temperature escalated, the amorphous phase remained unchanged up

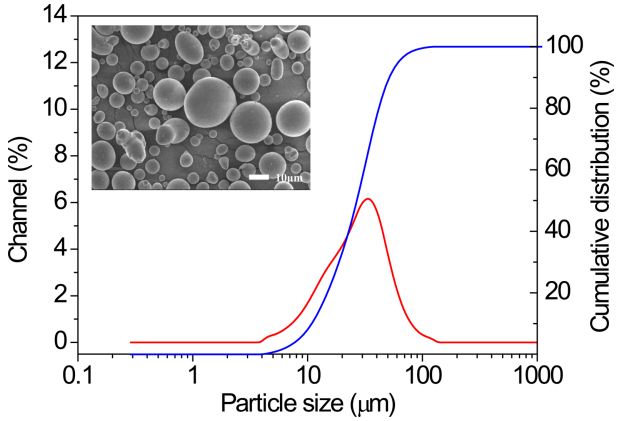

Fig. 1. (Color online) The particle size distribution of Fe-Cu-Nb-Si-B amorphous powders. Inserts shows SEM images illustrating the morphology.

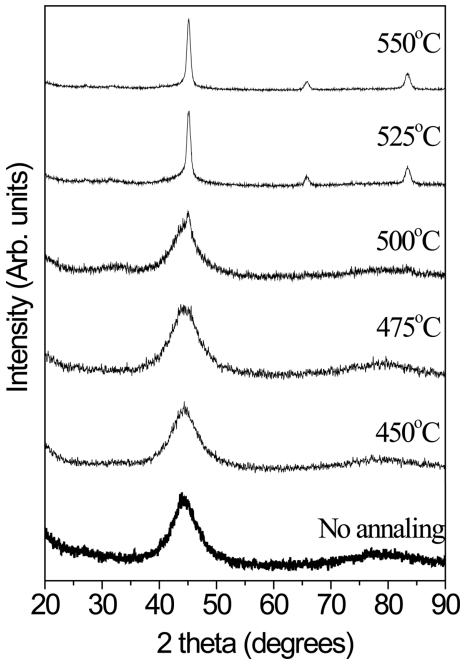

Fig. 2. X-ray diffraction patterns of Fe-Cu-Nb-Si-B amorphous powders as a function of heat treatment temperature.

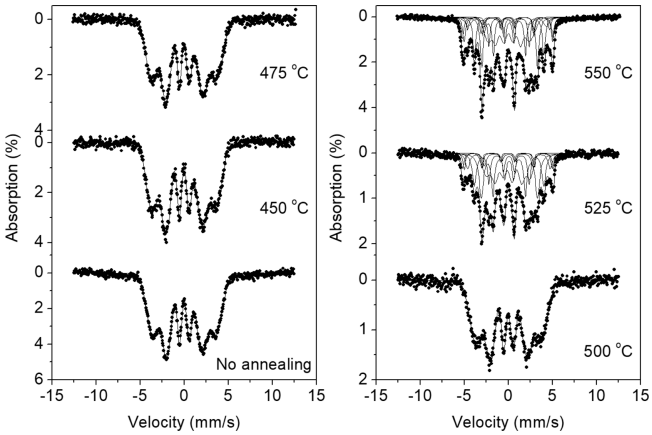

Fig. 3. Mössbauer analysis results at room temperature of Fe-Cu-Nb-Si-B amorphous powder as a function of heat treatment temperature. Powders that underwent heat treatment at temperatures below 500 °C exhibit amorphous behavior in the Fe-Cu-Nb-Si-B materials. In contrast, powders treated at 525 and 550 °C display a combination of amorphous and crystalline behavior.

to 475 °C, where a faint crystalline peak emerged. However, at 500 °C, the crystalline features were not sufficiently pronounced to permit detailed X-ray analysis. In order to ascertain the precise nature of the sample annealed at 500 °C, Mössbauer spectroscopy can be employed to discern whether it exhibits amorphous or crystalline characteristics. For powders annealed at 525 °C and 550 °C, a notably distinct X-ray phase was observed, diverging from the patterns observed at temperatures below 500 °C. The XRD analysis conclusively identified these powders as crystalline. Nevertheless, the determination of whether the powders annealed at 525 °C and 550 °C are entirely crystalline or if they incorporate amorphous phases remains challenging. Mössbauer spectroscopy offers the means to further investigate and elucidate the presence of mixed amorphous and crystalline phases or confirm the presence of entirely crystalline phases in these materials.

The Mössbauer spectra, recorded at room temperature for the Fe-Cu-Nb-Si-B amorphous powder subjected to varying heat treatment temperatures, are depicted in Fig. 3. In line with the findings from X-ray analysis, the Fe-Cu-Nb-Si-B powder subjected to heat treatment temperatures below 500 °C exhibited an amorphous Mössbauer spectrum, and the corresponding analysis results are succinctly presented in Table 1. For powders annealed at 525 and 550 °C, a complex interplay of crystalline and amorphous materials was evident, as indicated in Table 2. Notably, in the X-ray diffraction analysis, the powders treated at 525 and 550 °C exhibited peaks suggestive of crystalline phases, whereas Mössbauer analysis revealed a nuanced composition. Specifically, at 525 °C, Mössbauer analysis identified the presence of α-Fe, α-FeSi, Fe_2Si, and Fe_3Si, with Fe_3Si distributed across two distinct *A* and *B* sites. The analysis delineated five sextets and one amorphous peak in this configuration. Upon annealing at 550 °C, the Mössbauer analysis unveiled an additional Fe_2B site compared to the 525 °C treatment, characterized by six

Table 1. Hyperfine field H_{hf}, quadrupole splitting ΔE_Q, isomer shift δ, saturation magnetic moment M_S and coercivity H_C for Fe-Cu-Nb-Si-B amorphous powders annealed at various temperatures measured at room temperature (RT).

Annealing Temperature (°C)	H_{hf} (kOe)	ΔE_Q (mm/s)	δ (mm/s)	M_S (emu/g)	H_C (Oe)
As-annealed	221.36	0.00	0.02	131.23	4.26
450	230.66	0.01	-0.03	137.52	3.71
475	229.32	0.00	0.02	136.56	3.67
500	227.05	-0.01	0.00	136.21	3.65

Table 2. Hyperfine field H_{hf}, quadrupole splitting ΔE_Q, isomer shift δ for iron oxide nanoparticles annealed at 150 ℃ and pre-heat powders measured at 4.2 K and room temperature (RT).

Annealing Temperature (°C)	Site	H_{hf} (kOe)	E_Q (mm/s)	δ (mm/s)	A (%)
550	α-Fe	319.39	0.03	-0.10	8.67
	α-FeSi	311.39	-0.01	-0.01	9.50
	Fe_2Si	289.18	0.01	0.02	4.65
	Fe_2B	275.83	0.11	-0.24	7.81
	Fe_3Si_*A*-site	244.76	0.00	0.08	16.45
	Fe_3Si_*B*-site	195.83	0.01	0.13	21.88
	Amorphous	144.37	0.05	0.15	31.04
525	α-Fe	316.18	-0.06	-0.04	6.61
	α-FeSi	314.09	0.07	-0.03	5.97
	Fe_2Si	290.70	0.02	0.04	9.79
	Fe_3Si_*A*-site	244.67	0.01	0.07	15.62
	Fe_3Si_*B*-site	198.05	0.01	0.10	23.06
	Amorphous	152.25	-0.01	-0.03	38.95

sextets and one amorphous peak. Consequently, it is discernible that the transition from the amorphous to crystalline phase occurs as the heat treatment temperature of the Fe-Cu-Nb-Si-B amorphous powder is elevated. The Mössbauer spectroscopy outcomes thus illuminate the intricate evolution of the material's structural composition during heat treatment, offering invaluable insights into the interplay between crystalline and amorphous phases at elevated temperatures. These findings contribute to an enhanced understanding of phase transformations within the Fe-Cu-Nb-Si-B system and emphasize the pivotal role played by Mössbauer analysis in characterizing such intricate material transformations. The powder annealed at 525 °C was analyzed, revealing an approximate composition of 39 % amorphous and 61 % crystalline phases. In contrast, the powder annealed at 550 °C exhibited an approximate composition of 31 % amorphous and 69 % crystalline phases. At 525 °C, boron contributes to the amorphous phase, whereas at 550 °C, it also participates in the crystalline phase as Fe_2B. The crystalline phase primarily identified at 525 °C comprises Fe-Si. With a further increase in the heat treatment temperature, a phase transition occurs, progressing from amorphous to fully crystalline.

Figure 4 shows the hyperfine field analysis of Fe-Cu-Nb-Si-B powder at room temperature as a function of heat treatment temperature. In the case of the 525 and 550 °C powders, a mixture of amorphous and crystalline phases is observed, and consequently, only the hyperfine field values corresponding to the amorphous phase are depicted in Fig. 4. It is evident that as the heat treatment

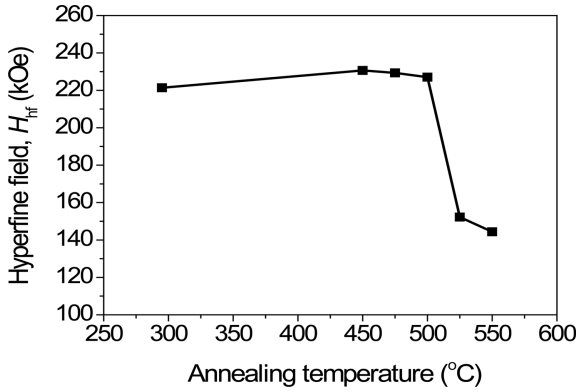

Fig. 4. Hyperfine magnetic field values of Fe-Cu-Nb-Si-B amorphous powder at different heat treatment temperatures. In particular, this figure shows the hyperfine field values for the amorphous phase of the sample annealed at 525 and 550 degrees Celsius. Since the crystalline and amorphous phases are mixed, the values for the amorphous phase are shown in the figure to show the behavior of the amorphous phase.

temperature increases, there is a slight initial increase in the hyperfine field, followed by a sharp decline at 525 °C. This phenomenon is attributed to the reduction of the amorphous phase as it transforms into both crystalline and amorphous phases. Notably, the untreated powder exhibited a value of 221.36 kOe, while the powder annealed at 450 °C demonstrated the highest value at 230.66 kOe. The quadrupole splitting value approaches nearly zero, and the isomer shift value indicates that Fe is present as an ionic alloy.

Saturation magnetization and coercive force measure-

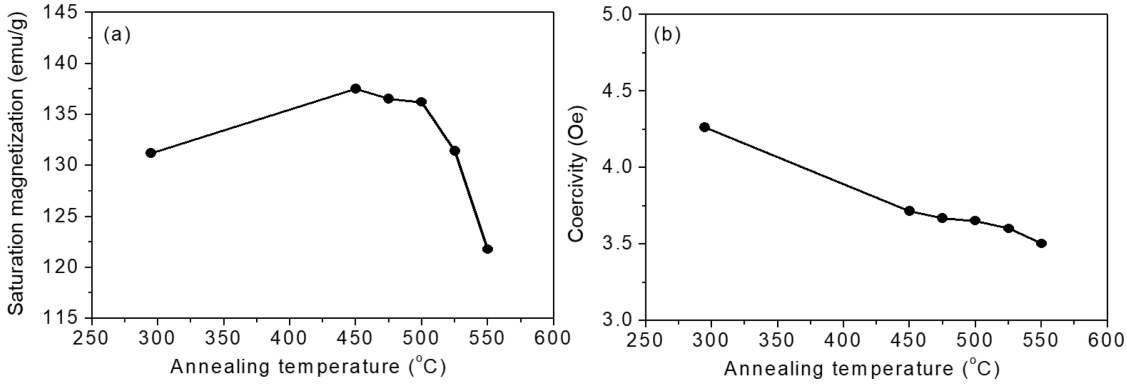

Fig. 5. (a) Saturation magnetization and (b) coercivity values as a function of heat treatment temperature for amorphous Fe-Cu-Nb-Si-B powder. Measurements were made at room temperature and an external magnetic field of 10 kOe was applied.

ments were conducted on Fe-Cu-Nb-Si-B amorphous powder as a function of heat treatment temperature, applying an external magnetic field of 10 kOe. The obtained results are presented in Fig. 5. The saturation magnetization value for the untreated powder was 131.2 emu/g. Notably, as the heat treatment temperature increased, there was a corresponding increase in the saturation magnetization value. However, a significant drop was observed starting at 525 °C, coinciding with the emergence of the crystalline phase. The value decreased to 121.8 emu/g for the sample treated at 550 °C. It's worth noting that a larger saturation magnetization value signifies a higher current-carrying capacity for the metal magnetic powder. Therefore, it is advisable to maintain a high saturation magnetization value, making the 500 °C temperature treatment, just before the crystalline phase transition, the most suitable. Regarding coercive force, it is evident that it decreases with increasing heat treatment temperature. A smaller coercive force is recommended as it can minimize losses in electronic components.

The temperature-dependent magnetic moment values of the Fe-Cu-Nb-Si-B amorphous powder were systematically measured and are depicted in Fig. 6. As the temperature increased, the magnetic moment value remained relatively stable until a sharp decline was observed at 823 K. This transition revealed the presence of two distinct Curie temperatures, denoted as T_C1 and T_C2, which were determined using the dM/dT curve. T_C1 was established at 845 K, while T_C2 occurred at 955 K. The latter, T_C2, represents the temperature at which the material entirely loses its magnetism. It is noteworthy that a spin rearrangement takes place between T_C1 and T_C2, leading to a disordered spin configuration above 955 K, resulting in the loss of magnetism.

To assess the feasibility of using the metal powder at high frequencies, we conducted permeability measurements

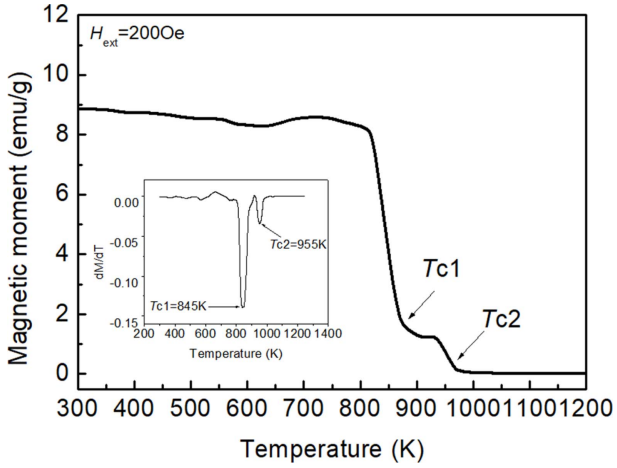

Fig. 6. M-T curve of amorphous Fe-Cu-Nb-Si-B powder with external magnetic field 200 Oe. The inset shows a dM/dT curve to determine the Curie temperature.

across a frequency range spanning from 0.1 MHz to 110 MHz. Figure 7(a) displays the measured permeability values in relation to frequency. These measurements were conducted after preparing an amorphous ribbon with the same composition as the Fe-Cu-Nb-Si-B amorphous powder and coiling the ribbon into a toroidal shape. Additionally, in Fig. 7(b), we examined a magnetic composite sample in the form of a toroid by incorporating 2.5 wt% of Fe-Cu-Nb-Si-B amorphous powder and epoxy binder, which underwent heat treatment at 500 °C. A copper wire was wound around it ten times, and impedance measurements were conducted using an impedance analyzer. Directly utilizing metal magnetic materials within the frequency range of 1 to 10 MHz, typical for power inductors, is challenging due to the constraints posed by the Snoek effect [6]. To circumvent this limitation, the use of a composite comprising metal magnetic powder and epoxy is necessary. Figure 7(a)

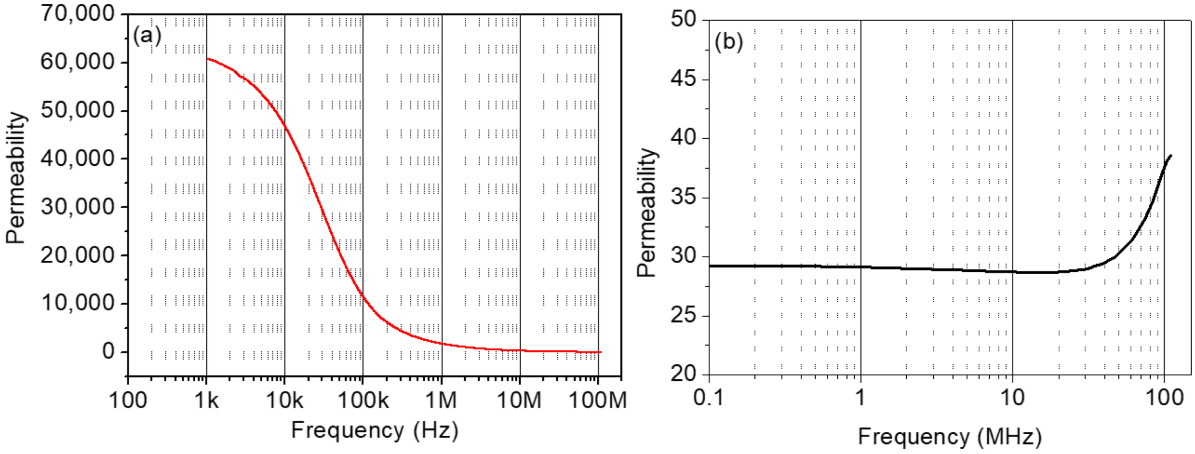

Fig. 7. (Color online) (a) Permeability graph of Fe-Cu-Nb-Si-B amorphous ribbon as a function of frequency and (b) Permeability graph of Fe-Cu-Nb-Si-B amorphous composite toroidal core as a function of frequency. It is evident that the metal magnetic composite exhibits a permeability exceeding 60,000 at 1 kHz, whereas the composite alone possesses a permeability value of 28 at the same frequency. The incorporation of the metal powder into an epoxy binder substantially reduces the permeability, rendering it suitable for high-frequency applications beyond 1 MHz.

illustrates the permeability behavior of the Fe-Cu-Nb-Si-B amorphous ribbon, indicating a permeability exceeding 60,000 at 1 kHz. However, as the frequency increases, the permeability experiences a rapid decline. Moreover, deploying metal powder at high frequencies presents difficulties due to increased core loss attributed to eddy currents. In contrast, Fig. 7(b) showcases a composite of metal magnetic particles. Here, the permeability remains remarkably consistent within the frequency range of 1 MHz to 10 MHz, maintaining a value of 28. A pronounced increase in permeability is observed at frequencies exceeding 40 MHz. This composite of metal magnetic powders demonstrates its suitability for high-frequency applications. By identifying the appropriate heat treatment temperature just before the amorphous-to-crystalline phase transition and conducting heat treatment to mitigate core losses while enhancing magnetic properties, the potential for high-frequency applications can be further realized.

4. Conclusion

In this study, heat treatments were conducted on Fe-Cu-Nb-Si-B amorphous powders in a vacuum environment to investigate their crystal structure and magnetic properties. The primary objective was to assess the viability of utilizing these soft metallic magnetic powders in high-frequency electronic applications. The study unveiled a phase transition from an amorphous to a crystalline state as the heat treatment temperature increased. This transition led to the emergence of a mixed phase comprising both amorphous and crystalline components at elevated temperatures, significantly influencing the material's magnetic behavior. Mössbauer spectroscopy was employed to characterize this transition, providing valuable insights into the distinct compositions of the crystalline and amorphous mixed phases at temperatures of 525 and 550 °C. Further examination of the magnetic properties unveiled a noteworthy trend in saturation magnetization values. Initially, there was an observed increase in magnetization with rising heat treatment temperatures. However, beyond 525 °C, a decline in magnetization became evident, aligning with the material's decomposition into multiple crystalline phases. The identification of two distinct Curie temperatures, T_C1=845 K (572 °C) and T_C2=955 K (682 °C), underscored the intricate nature of the magnetic transitions inherent in this material. The potential utility of amorphous Fe-Cu-Nb-Si-B powders in high-frequency electronic applications, where the mitigation of eddy-current losses holds paramount importance, appears promising. Notably, the superior saturation magnetization of these powders in comparison to conventional spinel ferrites positions them as compelling candidates for chip power inductors, particularly when operating at frequencies surpassing 1 MHz. Furthermore, envisioning the incorporation of these powders into composite materials within polymer matrices presents an exciting avenue to extend their applicability into higher frequency ranges by fine-tuning their magnetic resonance frequencies accordingly. In conclusion, this study has unveiled valuable insights into the crystallographic and magnetic properties of amorphous Fe-Cu-Nb-Si-B powders,

highlighting their potential for high-frequency electronic applications. These findings lay the foundation for the development of innovative materials poised to revolutionize the landscape of modern electronic devices. As the study concludes, anticipation for further exploration in this field grows, where untapped potential awaits, and these materials may pave the way for groundbreaking advancements in high-frequency electronic technologies.

Acknowledgements

The author would like thank Prof. Chul Sung Kim in Kookmin university for helping in Mössbauer measurements. This paper is written with support for research funding from aSSIST University.

Compliance with Ethical Standards

Conflict of interest: The author declare that they have no conflict of interest.

References

[1] N. V. Ilin, S. V. Komogortsev, G. S. Kraynova, A. V. Davydenko, I. A. Tkachenkon, A. G. Kozlov, V. V. Tkachev, and V. S. Plotnikov, J. Magn. Magn. Mater. **541**, 168525 (2022).
[2] J. Zhou, J. You, and K. Qiu, J. Appl. Phys. **132**, 040702 (2022).
[3] P. Gramatyka, R. Nowosielski, and P. Sakiewicz, J. Achiev. Mater. Manufac. Eng. **20**, 115 (2007).
[4] T. Larimian, V. Chaudhary, M. U. F. Khan, R. V. Ramanujan, R. K. Gupta, and T. Borkar, Intermetallics **129**, 107035 (2021).
[5] A. Makino, IEEE Trans. Magn. **48**, 1331 (2012).
[6] C. Jiang, S. S. Ghosh, H. Zhao, Y. Shen, and T. Long, IEEE Trans. Power Electron. **35**, 10821 (2020).
[7] H. Hsiang, J. Mater. Sci.: Mater. Electro. **31**, 16089 (2020).
[8] H. Kim and S. Y. An, J. Magn. **20**, 138 (2015).
[9] K. Shiroki, K. Kawano, H. matsuura, and H. Kishi, J. Jpn. Soc. Powder Powder Metallurgy **61**, S242 (2014).
[10] J. L. Snoek, Physica **14**, 207 (1948).
[11] A. N. Lagarkov and K. N. Rozanov, J. Magn. Magn. Mater. **321**, 2082 (2009).
[12] Y. J. Choi, J. H. Ahn, S. W. Kim, Y. R. Kim, and B. W. Lee, MRS Communications **11**, 457 (2021).
[13] S. Y. An, Journal of Radioanalytical and Nuclear Chemistry, (2023). https://doi.org/10.1007/s10967-023-08984-4
[14] T. Zhao, C. Chen, X. Wu, C. Zhang, A. A. Volinsky, and J. Hao, J. Alloys and Compounds **857**, 157991 (2021).
[15] E. A. Golovachev and S. A. Pakhomova, Journal of Physics: Conference Series **1990**, 012002 (2021).
[16] T. Gunes, Metallurgical and Materials Transactions A **50**, 4480 (2019).